A high precision phase reconstruction algorithm for multi-laser guide stars adaptive optics

2016 Chinese Phys. B 25 094214

(http://iopscience.iop.org/1674-1056/25/9/094214)

Chin. Phys. B Vol. 25, No. 9 (2016) 094214

SPECIAL TOPIC — Physical research in liquid crystal

A high precision phase reconstruction algorithm for multi-laser guide stars adaptive optics*

Bin He(何斌)[1,2], Li-Fa Hu(胡立发)[1,†], Da-Yu Li(李大禹)[1], Huan-Yu Xu(徐焕宇)[1], Xing-Yun Zhang(张杏云)[1], Shao-Xin Wang(王少鑫)[1], Yu-Kun Wang(王玉坤)[1], Cheng-Liang Yang(杨程亮)[1], Zhao-Liang Cao(曹召良)[1], Quan-Quan Mu(穆全全)[1], Xing-Hai Lu(鲁兴海)[1], and Li Xuan(宣丽)[1]

[1] *State Key Laboratory of Applied Optics, Changchun Institute of Optics, Fine Mechanics and Physics, Chinese Academy of Sciences, Changchun* 130033, *China*

[2] *University of Chinese Academy of Sciences, Beijing* 100039, *China*

(Received 18 May 2016; published online 19 July 2016)

Adaptive optics (AO) systems are widespread and considered as an essential part of any large aperture telescope for obtaining a high resolution imaging at present. To enlarge the imaging field of view (FOV), multi-laser guide stars (LGSs) are currently being investigated and used for the large aperture optical telescopes. LGS measurement is necessary and pivotal to obtain the cumulative phase distortion along a target in the multi-LGSs AO system. We propose a high precision phase reconstruction algorithm to estimate the phase for a target with an uncertain turbulence profile based on the interpolation. By comparing with the conventional average method, the proposed method reduces the root mean square (RMS) error from 130 nm to 85 nm with a 30% reduction for narrow FOV. We confirm that such phase reconstruction algorithm is validated for both narrow field AO and wide field AO.

Keywords: laser guide star, adaptive optics, phase reconstruction, liquid crystal wavefront corrector

PACS: 42.68.Wt, 42.66.Lc, 42.70.Df **DOI:** 10.1088/1674-1056/25/9/094214

1. Introduction

Adaptive optics (AO) technology is widely used to correct the distorted wavefront induced by atmospheric turbulence in real time, and restore the imaging resolution close to the diffraction limit of a telescope.[1] As an efficient wavefront corrector, phase-only liquid crystal on silicon (LCOS) possesses a prominent advantage of high pixel density, which makes it possible to be used in the AO system for large aperture telescopes.[2–7] To obtain images reaching the diffraction limit, a bright source such as a guide star must be available within the isoplanatic patch for aberration measurement. However, the brightness requirement is quite rigorous for arbitrary sky/space objects, which results in a low probability of finding a sufficient number of bright nature guide stars (NGSs) for AO correction. A solution to avoid the scarcity of bright NGSs is to produce artificial laser guide stars (LGS) from the ground by using the back-scattered (or back-radiated) light.[8] Thus, only one NGS is required to sense overall tilt since very faint NGS can still be used for image motion sensing. Several LGSs are used for high order aberration sensing in LGS AO systems.

Unfortunately, a light cone rather than a desired cylinder is produced from the LGS to the telescope, thereby resulting in an error called "focus anisoplanatism" (FA) or the cone effect. This is a serious impediment to the general application of LGS in large aperture telescope AO systems. Foy and Labeyrie in 1985 suggested to use an array of laser beacons for astronomical AO to reduce the FA error.[9,10] In their concept, the cumulative phase distortion along a target can be obtained solely from the LGS measurements. There are some works for this problem,[11–14] but all of these approaches have one aspect in common in that they require a priori knowledge of a real-time-varied profile. Hart proposed an approach for ground layer AO (GLAO) that the signals from the all beacons are sensed separately and averaged to obtain the mean wavefront as the estimation of the aberration.[15–17] In this approach, the weight factors of all LGSs are the same. However, as the FA error depends on the propagation path, it should be different for every LGS so that the weight factors should also be different. To resolve this problem and decrease the wavefront tomographic error, we propose a novel algorithm to calculate these weight coefficients based on the interpolation, and thereby estimate the phase for target without the measurement of the atmospheric turbulence refractive index structure constant C_n^2 profile. This method is simpler and obvious more accurate than the previous proposed ones. It can be predicted to be efficient to improve the imaging resolution in large FOV observation for GLAO with LGSs.

In this paper, the phase reconstruction algorithm is de-

*Project supported by the National Natural Science Foundation of China (Grant Nos. 11174274, 11174279, 61205021, 11204299, 61475152, and 61405194) and State Key Laboratory of Applied Optics, Changchun Institute of Optics, Fine Mechanics and Physics, Chinese Academy of Sciences.

†Corresponding author. E-mail: hulifa@ciomp.ac.cn

scribed in detail theoretically, and is then validated in simulation. The algorithm of phase reconstruction is presented in Section 2. We compare the simulation results and performances with the previous reported ones and analyze them in Section 3. Finally, the conclusions are given in Section 4.

2. Theory

2.1. Phase reconstruction

Assume that there are n different LGSs located at height H. $\boldsymbol{r}_i$ is the projected vector of the i-th LGS on the telescope aperture as shown in Fig. 1. An arbitrary point on the trace of a light (dashed line) emitted from the i-th LGS to point $\boldsymbol{r}$ has a position $(\boldsymbol{r} - z\boldsymbol{r}/H + z\boldsymbol{r}_i/H,\ z)$. According to the near-field approximation, the aberrated wavefront measured for this LGS is calculated as

$$\phi_i(\boldsymbol{r}) = \frac{2\pi}{\lambda}\int n\left(\frac{H-z}{H}\boldsymbol{r} + \frac{z}{H}\boldsymbol{r}_i, z\right)\mathrm{d}z, \tag{1}$$

where $n(\boldsymbol{r}, z)$ is the refractive index fluctuation along the beam at altitude z, and λ is the wavelength as convention.

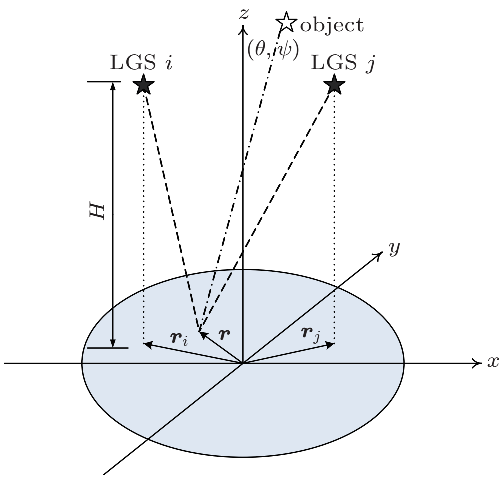

Fig. 1. (color online) Schematic diagram of LGSs' distribution and objective star with elevation angle θ and azimuth angle ψ. Light from LGS: dashed line; light from objective star: dot-dashed line.

The direction vector of a light from an objective star can be described as $(\cos\theta\cos\psi,\ \cos\theta\sin\psi,\ \sin\theta)$. Define a vector in the xy plane as $\boldsymbol{r}_\mathrm{o} = H\cos\theta\cos\psi\boldsymbol{e}_x + H\cos\theta\sin\psi\boldsymbol{e}_y$, where $\boldsymbol{e}_x$ and $\boldsymbol{e}_y$ are the unit vectors along the x and y axes, respectively. The position of an arbitrary point on the trace of the light (dot-dashed line) emitted from the object to point $\boldsymbol{r}$ is $(\boldsymbol{r} + z\boldsymbol{r}_\mathrm{o}/H, z)$. An aberrated wavefront is produced when a light emitted from the beacon (with a quasi-infinite distance from the project plane) passes through different atmospheric turbulence layers as shown in Fig. 1. Therefore, the optical path fluctuation is expressed as

$$\phi_\mathrm{o}(r) = \frac{2\pi}{\lambda}\int n\left[\boldsymbol{r} + \frac{z}{H}\boldsymbol{r}_\mathrm{o}, z\right]\mathrm{d}z. \tag{2}$$

According to the Kolmogorov theory, the turbulence field is a locally uniform and isotropic field. Its statistical properties are independent of the space position within the limited space. Therefore, the statistical aberration moments c and their corresponding square values σ_ϕ^2 at any point are the same

$$\langle\phi_\mathrm{o}\rangle = \langle\phi_i\rangle = c, \tag{3}$$
$$\left\langle\phi_\mathrm{o}^2\right\rangle = \left\langle\phi_i^2\right\rangle = \sigma_\phi^2. \tag{4}$$

We estimate the unknown aberration from the target star along the direction (θ, ψ) by the weighted summation of the detected data. The phase delay at any point on the telescope pupil can be estimated by the interpolation of n phase values measured from LGSs at the same point

$$\tilde{\phi}_\mathrm{o}(\boldsymbol{r}) = \sum_{i=1}^{n} k_i\phi_i(\boldsymbol{r}), \tag{5}$$

where k_i is the weight coefficient. This constitutes an array of optimal coefficients that minimizes the difference between the real value and the estimated value. It should meet the unbiased estimation constraint

$$\left\langle\sum_{i=1}^{n} k_i\phi_i - \phi_\mathrm{o}\right\rangle = 0. \tag{6}$$

According to Eq. (3) we have

$$\sum_{i=1}^{n} k_i = 1. \tag{7}$$

2.2. Determination of weight coefficients

To find an array of optimized weight coefficients, we have to analyze the estimation error J, expanded as the following polynomial, at first:

$$\begin{aligned} J &= \left\langle\left(\sum_{i=1}^{n} k_i\phi_i - \phi_\mathrm{o}\right)^2\right\rangle \\ &= \left\langle\left(\sum_{i=1}^{n} k_i\phi_i\right)^2\right\rangle - 2\left\langle\phi_\mathrm{o}\sum_{i=1}^{n} k_i\phi_i\right\rangle + \left\langle\phi_\mathrm{o}^2\right\rangle \\ &= \sum_{i=1}^{n}\sum_{j=1}^{n} k_ik_j\left\langle\phi_i\phi_j\right\rangle - 2\sum_{i=1}^{n} k_i\left\langle\phi_\mathrm{o}\phi_i\right\rangle + \left\langle\phi_\mathrm{o}^2\right\rangle \\ &= \sum_{i=1}^{n}\sum_{j=1}^{n} k_ik_j\left(\sigma_\phi^2 - \frac{1}{2}D_{ij}\right) \\ &\quad - 2\sum_{i=1}^{n} k_i\left(\sigma_\phi^2 - \frac{1}{2}D_{\mathrm{o}i}\right) + \sigma_\phi^2, \end{aligned} \tag{8}$$

where $D_{\mathrm{o}i}$ is the variance of the difference between ϕ_o and ϕ_i, and D_{ij} is the variance of the difference between ϕ_i and ϕ_j. They can be calculated directly from the Kolmogorov structure function as follows:

$$\begin{aligned} D_{\mathrm{o}i}(\boldsymbol{r}) &= \left\langle[\phi_i(\boldsymbol{r}) - \phi_\mathrm{o}(\boldsymbol{r})]^2\right\rangle \\ &= 2.91\left(\frac{2\pi}{\lambda}\right)^2\int\left|-\frac{z}{H}\boldsymbol{r} + \frac{z}{H}\boldsymbol{r}_i - \frac{z}{H}\boldsymbol{r}_\mathrm{o}\right|^{5/3} C_n^2(z)\,\mathrm{d}z \end{aligned}$$

$$= |\boldsymbol{r}_\mathrm{o}+\boldsymbol{r}-\boldsymbol{r}_i|^{5/3}/(\theta_0 H)^{5/3}, \tag{9}$$

$$\begin{aligned} D_{ij}(\boldsymbol{r}) &= \left\langle [\phi_j(\boldsymbol{r})-\phi_i(\boldsymbol{r})]^2 \right\rangle \\ &= 2.91\left(\frac{2\pi}{\lambda}\right)^2 \int \left|(\boldsymbol{r}_j-\boldsymbol{r}_i)\frac{z}{H}\right|^{5/3} C_n^2(z)\,\mathrm{d}z \\ &= \left|\boldsymbol{r}_j-\boldsymbol{r}_i\right|^{5/3}/(\theta_0 H)^{5/3}, \end{aligned} \tag{10}$$

where $C_n^2(z)$ is the structure constant of refractive index at altitude z, while θ_0 is the isoplanatic angle of the atmosphere. Substituting Eq. (7) into Eq. (8), we arrive at

$$J=\sum_{i=1}^{n}k_i D_{\mathrm{o}i}-\frac{1}{2}\sum_{i=1}^{n}\sum_{j=1}^{n}k_i k_j D_{ij}. \tag{11}$$

The optimization of J under the constraint of Eq. (6) can be solved with the Lagrange multiplier method. We construct a new objective function for the optimization

$$J'=J+\gamma\left(\sum_{i=1}^{n}k_i-1\right), \tag{12}$$

where γ is a Lagrange multiplier. Find a series of parameters $\{\gamma,\ k_1,\ k_2,\dots,k_n\}$ to minimize the function J on the condition of Eq. (6), which can be determined by solving the following partial differential equations:

$$\begin{cases} \dfrac{\partial J'}{\partial k_i}=0, \quad (i=1,2,\dots,n), \\ \dfrac{\partial J'}{\partial \gamma}=0. \end{cases} \tag{13}$$

Substituting Eqs. (9)–(12) into Eq. (13), we arrive at

$$\begin{cases} \gamma+\sum\limits_{j=1}^{n}\left|\boldsymbol{r}_j-\boldsymbol{r}_i\right|^{5/3}k_j=|\boldsymbol{r}_\mathrm{o}+\boldsymbol{r}_i-\boldsymbol{r}|^{5/3}, \quad (i=1,2\cdots n), \\ \sum\limits_{j=1}^{n}k_j=1. \end{cases} \tag{14}$$

Its matrix formation is given as

$$\begin{bmatrix} d_{11} & d_{12} & \cdots & d_{1n} & 1 \\ d_{21} & d_{22} & \cdots & d_{2n} & 1 \\ \vdots & \vdots & \ddots & \vdots & \vdots \\ d_{n1} & d_{n2} & \cdots & d_{nn} & 1 \\ 1 & 1 & \cdots & 1 & 0 \end{bmatrix} \begin{bmatrix} k_1 \\ k_2 \\ \vdots \\ k_n \\ \gamma \end{bmatrix} = \begin{bmatrix} d_{\mathrm{o}1} \\ d_{\mathrm{o}2} \\ \vdots \\ d_{\mathrm{o}n} \\ 1 \end{bmatrix}, \tag{15}$$

where $d_{ij}=|\boldsymbol{r}_j-\boldsymbol{r}_i|^{5/3}$ and $d_{\mathrm{o}i}=|\boldsymbol{r}_\mathrm{o}+\boldsymbol{r}-\boldsymbol{r}_i|^{5/3}$. Solve the matrix equation (15), and the weight coefficients k_i can be obtained. The weight coefficients depend on the location of the point $\boldsymbol{r}$, the direction along the objective star and its corresponding projected vectors of LGS, $\boldsymbol{r}_i$, are independent of C_n^2

2.3. Optimization of LGS position

LGSs are generally arranged in regular polygon. We consider 6 LGSs that are arranged at the vertices of a hexagon as shown in Fig. 2(a). The distance ρ between each LGS and the center is the same. θ_{fov} is the diameter of FOV. The estimation error $J(\boldsymbol{r}_\mathrm{o},\boldsymbol{r})$ is related to ρ. We choose an optimized ρ to minimize the aperture-averaged error. The aperture-averaged error J_m is defined as

$$\begin{aligned} J_\mathrm{m} &= \frac{16}{\pi^2 D^2 L^2}\iint\limits_{|\boldsymbol{r}|\le D/2}\mathrm{d}\boldsymbol{r}\iint\limits_{|\boldsymbol{r}_\mathrm{o}|\le L/2} J(\boldsymbol{r}_\mathrm{o},\boldsymbol{r})\,\mathrm{d}\boldsymbol{r}_\mathrm{o} \\ &= \frac{16}{\pi^2 D^2 L^2}\left(\frac{1}{\theta_0 H}\right)^{5/3} \\ &\quad\times \iint\limits_{|\boldsymbol{r}|\le D/2}\mathrm{d}\boldsymbol{r}\iint\limits_{|\boldsymbol{r}_\mathrm{o}|\le L/2}\left(\sum_{i=1}^{n}k_i\left|\boldsymbol{r}_i+\boldsymbol{r}_\mathrm{o}-\boldsymbol{r}\right|^{5/3}\right. \\ &\quad\left. -\frac{1}{2}\sum_{i=1}^{n}\sum_{j=1}^{n}k_i k_j\left|\boldsymbol{r}_j-\boldsymbol{r}_i\right|^{5/3}\right)\mathrm{d}\boldsymbol{r}_\mathrm{o}. \end{aligned} \tag{16}$$

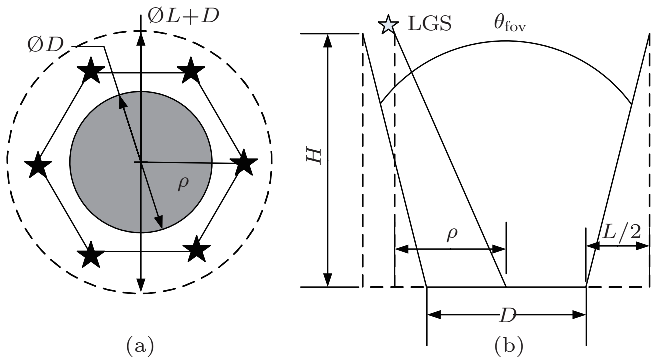

Fig. 2. Arrangement of six LGSs and their geometric relationship, $L=\theta_{\mathrm{fov}}H$: (a) plan view, (b) side view.

The results for J_m, which is a function of ρ, when $L=0$ are calculated and shown in Fig. 3. The results based on the proposed method are much smaller than those based on the average method whatever the ρ is. And the minimum J_m is reached at $\rho/D=0.37$ for both the proposed method and the average method.

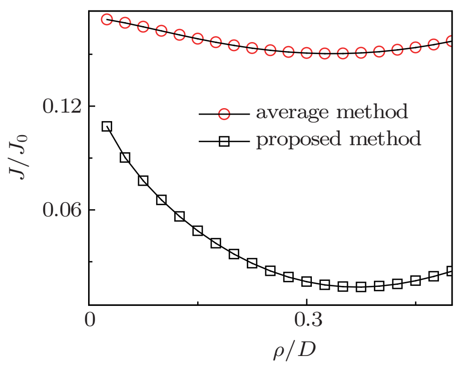

Fig. 3. (color online) The J_m varying with ρ. Here $J_0=(D/\theta_0 H)^{5/3}$.

For the same LGS, the weight coefficient changes with the location of the point in the aperture. Calculate the weight coefficient of each point over the telescope for each LGS. All the weight coefficients when $\rho/D=0.37$ are shown in Fig. 4. The circle region is the telescope aperture and the grey value represents the weight coefficient, which is ranged from 0 to 1.

Figure 4 indicates that the weight coefficient is large nearby the projection of the corresponding LGS. This is reasonable since a closer position to the projection of LGS generally leads to a smaller difference between the measured and the desired results. As a contrast, the weighted coefficient of the reported average method is $1/n$ at any point for any LGS.

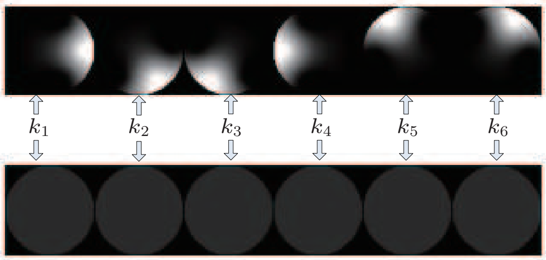

Fig. 4. The weighted coefficients comparison between the proposed method (top) and the average method (bottom) for $\rho = 0.37D$.

The optimal ρ for different FOVs are different. Figure 5 shows the optimal ρ normalized by the diameter D of the telescope.

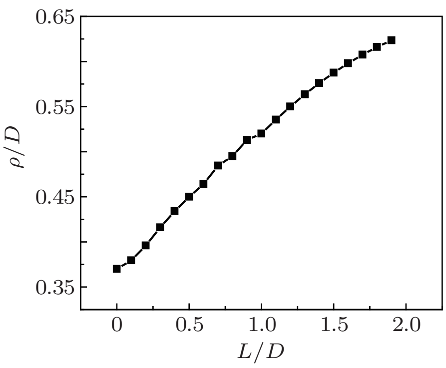

Fig. 5. Optimal ρ as a function of L.

3. Result

For this work, we have chosen to use the well-known Hufnagel–Valley 5/7 mode. Such profile Troxel determines that four layers can be used to accurately model the turbulence,[18] and the altitudes and strengths of the layers are listed in Table 1. The Fried parameter r_0 is 0.1 m at $\lambda = 500$ nm, and the outer scale of the atmosphere is 30 m.

Table 1. Altitudes and relative layer strengths of four-layer turbulence model.

Layer	1	2	3	4
Height/m	200	2000	10000	18000
Strength	0.8902	0.0443	0.0591	0.0064

In our simulation, a 6 m telescope is adopted with six LGSs at height 20 km. The positions of the LGSs have been shown in Fig. 2 and their zenith angles will be determined by FOV later. We use several wavefront sensors and one single liquid crystal wavefront corrector (LCWC)[19–23] optically conjugated to the telescope pupil. For simplification, the wavefront spatial sampling error induced by the wavefront sensor (WFS) and LCWC is ignored, and the performance of the AO system is limited only by the wavefront reconstruction algorithm. The above expression for J counts errors in sampling all modes of the distorted wavefront, including piston and tip/tilt. Herein, we only consider the error without piston and tip/tilt components by considering that the piston error is irrelevant to the Strehl ratio (SR) for a single aperture; besides, the global tip-tilt component is detected by NGS and compensated by the tilt mirror.[24,25]

3.1. Narrow FOV

We first consider a narrow FOV with $\theta_{\rm fov} = 0'$ so that the target is at an infinite distance and zenith direction. As aforementioned optimization, $L = 0$, and the optimal ρ is $0.37D = 2.22$ m. Therefore, the zenith angle of LGS is $18.3''$. The RMS after compensating is shown at Fig. 6. It is noteworthy that the proposed method reduces the RMS from 130 nm to 85 nm compared with the average method. The point spread function (PSF) at 1 μm wavelength in 500 ms integral time is shown at Fig. 7, revealing an obvious improvement of the SR from 0.49 to 0.75, which validates this method.

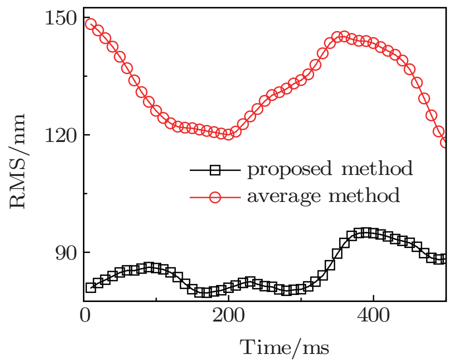

Fig. 6. (color online) Comparison of the reconstruction performance. The Greenwood frequency is 28.8 Hz.

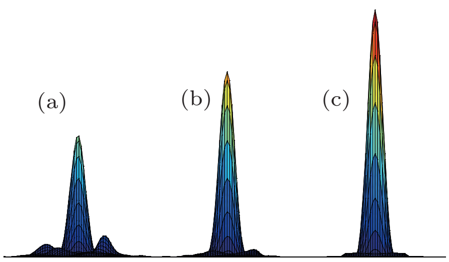

Fig. 7. (color online) The long-exposure (500 ms) at 1 μm with 6 LGSs: (a) average method (SR = 0.49), (b) the proposed method (SR = 0.75), (c) the diffraction limit.

3.2. Large FOV

This method is also applicable in the case of large FOV. Consider that the diameter of FOV is 1 arcmin. Thus, $L = 1.2D$, and the optimal ρ is $0.55D$, i.e., 3.3 m, from Fig. 5.

Therefore, the zenith angle of LGS is 27.2″. To improve the imaging quality by the partial correction of the low-altitude turbulence, an optimization in the whole FOV range is carried out based on a GLAO system. The LCWC is controlled by measuring six higher-order WFSs viewing guidestars. The interpolation coefficient along all directions in the FOV is calculated and averaged, respectively, and subsequently substituted into Eq. (5), consequently the final interpolation coefficient is obtained. Figure 8 displays SRs obtained by the average method (denoted by red hollow circle) and our proposed method (denoted by black hollow square). Apparently, the latter is better than the former within almost the entire FOV, especially near the center area of FOV. This confirms that the phase reconstruction method is validated for the wide field AO.

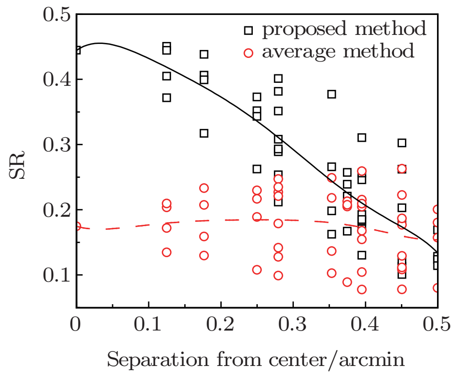

Fig. 8. (color online) Comparison of the proposed algorithm with the average method. Each point represents a view point within FOV. The solid and dash curves are their corresponding fitted results.

4. Conclusion and perspectives

In this paper, a phase reconstruction algorithm is proposed to estimate the phase for a target with an uncertain turbulence profile based on the interpolation. This algorithm is independent of the complicated measurement of turbulence C_n^2 profile. Compared with the conventional average method, the proposed method reduces the RMS from 130 nm to 85 nm with a 30% reduction for narrow FOV. In addition, it is applicable for the case of a larger FOV. The simulation results indicate that the phase reconstruction algorithm can obtain a higher imaging resolution for a large FOV.

References

[1] Booth M J 2014 *Light Sci. Appl.* **3** e165
[2] Xuan L, Li D Y and Liu Y G 2015 *Chin. J. Liq. Cryst. Disp.* **30** 1 (in Chinese)
[3] Min L, Yao L S, Wang Y K, Wang S X, Liu Y G, Peng Z H and Xuan L 2015 *Chin. J. Liq. Cryst. Disp.* **30** 32
[4] Wang Y C, Zhang Z D and Zhou X 2015 *Chin. J. Liq. Cryst. Disp.* **30** 949 (in Chinese)
[5] Yu Y, Zhou X and Zhang Z D 2015 *Chin. J. Liq. Cryst. Disp.* **30** 213 (in Chinese)
[6] Chen Y C, Xuan L, Yao L S and Peng Z H 2016 *Chin. J. Liq. Cryst. Disp.* **31** (in Chinese)
[7] Zhou Q, Lu J F and Yin J P 2013 *Chin. J. Liq. Cryst. Disp.* **28** 349 (in Chinese)
[8] McCall S and Passner A 1978 *Adaptive Optics and Short Wavelength Sources* **1** 149
[9] Fried D L 1995 *J. Opt. Soc. Am. A* **12** 939
[10] Foy R and Labeyrie A 1985 *Astron. Astrophys.* **152** L29
[11] Vidal F, Gendron E and Rousset G 2010 *J. Opt. Soc. Am. A* **27** 253
[12] Neichel B, Fusco T and Conan J M 2009 *J. Opt. Soc. Am. A* **26** 219
[13] Rosensteiner M and Ramlau R 2013 *J. Opt. Soc. Am. A* **30** 1680
[14] Fusco T, Conan J M, Michau V, Mugnier L M and Rousset G 1999 *Opt. Lett.* **24** 1472
[15] Hart M, Milton N M, Baranec C, Powell K, Stalcup T, McCarthy D, Kulesa C and Bendek E 2010 *Nature* **466** 727
[16] Baranec C, Hart M, Milton N M, Stalcup T, Powell K, Snyder M, Vaitheeswaran V, McCarthy D and Kulesa C 2009 *Astrophys. J.* **693** 1814
[17] Lloyd H M, Baranec C, Milton N M, Snyder M, Stalcup T and Angel J R P 2006 *Opt. Express* **14** 7541
[18] Troxel S E, Roggemann M C and Welsh B M 1994 *J. Opt. Soc. Am. A* **11** 2100
[19] Zhang Z, You Z and Chu D 2014 *Light Sci. Appl.* **3** e213
[20] Wang L, Lin X W, Hu W, Shao G H, Chen P, Liang L J, Jin B B, Wu P H, Qian H, Lu Y N, Liang X, Zheng Z G and Lu Y Q 2015 *Light Sci. Appl.* **4** e253
[21] Liu R X, Zheng X L, Li D Y, Xia M L, Hu L F, Cao Z L, Mu Q Q and Xuan L 2014 *Chin. Phys. B* **23** 94211
[22] Liu C, Mu Q Q, Hu L F, Cao Z L and Xuan L 2010 *Chin. Phys. B* **19** 64214
[23] Zhang Y C, Hu L F, Peng Z H and Xuan L 2014 *Chin. J. Liq. Cryst. Disp.* **29** 709 (in Chinese)
[24] Fan M W, Huang L H, Li M and Rao C H 2015 *Opt. Precis. Eng.* **23** 2803 (in Chinese)
[25] Wang Y K, H L F, Wang C C, Wang S X and Xuan L 2015 *Opt. Precis. Eng.* **23** 2203 (in Chinese)